2009

RF magnetron sputtered (BiDy)3(FeGa)5O12:Bi2O3 composite garnet-oxide materials possessing record magneto-optic quality in the visible spectral region

Mikhail Vasiliev
Edith Cowan University

Mohammad Alam
Edith Cowan University

V.A. Kotov

Kamal Alameh
Edith Cowan University

V.I. Belotelov

See next page for additional authors

Authors

Mikhail Vasiliev, Mohammad Alam, V.A. Kotov, Kamal Alameh, V.I. Belotelov, V.I. Burkov, and A.K. Zvezdin

RF magnetron sputtered $(BiDy)_3(FeGa)_5O_{12}$:Bi_2O_3 composite garnet-oxide materials possessing record magneto-optic quality in the visible spectral region

Mikhail Vasiliev,[1] Mohammad Nur-E-Alam,[1] Viacheslav A. Kotov,[2] Kamal Alameh,[1] Vladimir I. Belotelov,[3] Vladimir I. Burkov,[4] and Anatoly K. Zvezdin[5]

[1]*Electron Science Research Institute, Edith Cowan University, 270 Joondalup Drive, Joondalup, WA, 6027, Australia*
[2]*Institute of Radio Engineering and Electronics, Russian Academy of Sciences, 11 Mohovaya St, Moscow, 125009, Russia*
[3]*M.V. Lomonosov Moscow State University, Moscow 119992, Russia*
[4]*Moscow Institute of Physics and Technology, Dolgoprudny 141700, Russia*
[5]*A.M. Prokhorov Institute of General Physics, 38 Vavilov St, Moscow 119991, Russia*
*m.vasiliev@ecu.edu.au

Abstract: Bismuth-substituted iron garnets are considered to be the most promising magneto-optical materials because of their excellent optical transparency and very high magneto-optical figures of merit in the near-infrared spectral region. However, the practical application of garnets in the visible and short-wavelength infrared parts of spectrum is currently limited, due to their very high optical absorption (especially in sputtered films) in these spectral regions. In this paper, we identify the likely source of excess absorption observed in sputtered garnet films in comparison with epitaxial layers and demonstrate $(Bi,Dy)_3(Fe,Ga)_5O_{12}$: Bi_2O_3 composites possessing record MO quality in the visible region.

OCIS codes: (160.3820) Magneto-optical materials; (310.3840) Materials and process characterization; (130.3130) Integrated optics materials

References and links

1. G. B. Scott, and D. E. Lacklison, "Magnetooptic Properties and Applications of Bismuth Substituted Iron Garnets," IEEE Trans. Magn. **12**(4), 292–311, 292–311 (1976).
2. A. K. Zvezdin, and V. A. Kotov, in *Modern Magnetooptics and Magnetooptical Materials* (Institute of Physics Publishing, Bristol and Philadelphia, ISBN 075030362X, 1997).
3. T. Okuda, N. Koshizuka, K. Hayashi, T. Takahashi, H. Kotani, and H. Yamamoto, "Epitaxial growth of Bi-substituted yttrium iron garnet films by ion beam sputtering," Advances in Magneto-Optics, Proc. Int. Symp. Magneto-Optics, J. Magn. Soc. Jpn., **11**, Supplement S1, 179–182 (1987).
4. J.-P. Krumme, V. Doormann, B. Strocka, and P. Willich, "Selected-area sputter epitaxy of iron-garnet films," J. Appl. Phys. **60**(6), 2065–2068 (1986).
5. T. Okuda, T. Katayama, K. Satoh, T. Oikawa, H. Yamamoto, and N. Koshizuka, in Proceedings of the 5th Symposium on Magnetism and Magnetic Materials, Taipei, Taiwan, Ed. by H.L. Huang and P.C. Kuo (World Scientific, Singapore, 1990), p. 61.
6. T. Okuda, T. Katayama, K. Satoh, T. Oikawa, H. Yamamoto, and N. Koshizuka, "Preparation of polycrystalline $Bi_3Fe_5O_{12}$ garnet films," J. Appl. Phys. **69**(8), 4580–4582 (1991).
7. P. Hansen, W. Tolksdorf, K. Witter, and J. M. Robertson, "Recent advances of bismuth garnet materials research for bubble and magneto-optical applications," IEEE Trans. Magn. **20**(5), 1099–1104 (1984).
8. R. Ramesh, B.M. Simion and G. Thomas, "Epitaxial Magnetic Garnet Heterostructures," J. Phys. IV France **7,** C1–695 – C1–698 (1997).
9. B. Teggart, R. Atkinson, and I. W. Salter, "Enhancement of the polar Kerr effect in bismuth-substituted DyGa iron garnet thin films," J. Phys. D Appl. Phys. **31**(19), 2442–2446 (1998).
10. M. Inoue, K. Arai, T. Fuji, and M. Abe, "One-dimensional magnetophotonic crystals," J. Appl. Phys. **85**(8), 5768 (1999).
11. Y. H. Kim, J. S. Kim, S. I. Kim, and M. Levy, "Epitaxial Growth and Properties of Bi-Substituted Yttrium-Iron-Garnet Films Grown on (111) Gadolinium-Gallium-Garnet Substrates by Using rf Magnetron Sputtering," J. Korean Phys. Soc. **43**(3), 400–405 (2003).
12. S. Kahl, and A. M. Grishin, "Enhanced Faraday rotation in all-garnet magneto-optical photonic crystal," Appl. Phys. Lett. **84**(9), 1438 (2004).

13. S. I. Khartsev, and A. M. Grishin, "[Bi$_3$Fe$_5$O$_{12}$/Gd$_3$Ga$_5$O$_{12}$]^m magneto-optical photonic crystals," Appl. Phys. Lett. **87**, 122504 (2005).
14. S. I. Khartsev, and A. M. Grishin, "Heteroepitaxial Bi$_3$Fe$_5$O$_{12}$/La$_3$Ga$_5$O$_{12}$ films for magneto-optical photonic crystals," Appl. Phys. Lett. **86**, 141108 (2005).
15. R. Lux, A. Heinrich, S. Leitenmeier, T. Körner, M. Herbort, and B. Stritzker, "Pulsed-laser deposition and growth studies of Bi$_3$Fe$_5$O$_{12}$ thin films," J. Appl. Phys. **100**(11), 113511 (2006).
16. V.I. Belotelov, L.L. Doskolovich, A.K. Zvezdin, "Extraordinary magnetooptical effects and transmission through the metal-dielectric plasmonic systems," Phys. Rev. Lett., **98**, 77401(1–4) (2007).
17. M. Vasiliev, K. E. Alameh, V. A. Kotov, and Y. T. Lee, "Nanostructured Engineered Materials With High Magneto-Optic Performance for Integrated Photonics Applications," in Proc. IEEE PhotonicsGlobal@Singapore, 2008 (IPGC 2008), ISBN 9781424439010, *http://ieeexplore.ieee.org/stamp/stamp.jsp?arnumber=4781410&isnumber=4781297*.
18. M. Vasiliev, P. C. Wo, K. Alameh, P. Munroe, Z. Xie, V. A. Kotov, and V. I. Burkov, "Microstructural characterization of sputtered garnet materials and all-garnet magnetic heterostructures: establishing the technology for magnetic photonic crystal fabrication," J. Phys. D Appl. Phys. **42**(13), 135003 (2009).
19. P. C. Wo, P. R. Munroe, M. Vasiliev, Z. H. Xie, K. Alameh, and V. Kotov, "A novel technique for microstructure characterization of garnet films," Opt. Mater. in press., doi:10.1016/j.optmat.2009.07.025.
20. V. I. Belotelov, and A. K. Zvezdin, "Magneto-optical properties of photonic crystals," J. Opt. Soc. Am. B **22**(1), 286 (2005).
21. V. Goossens, J. Wielant, S. Van Gils, R. Finsy, and H. Terryn, "Optical properties of thin iron oxide films on steel," Surf. Interface Anal. **38**(4), 489–493 (2006).
22. F. Ilievski, T. Tepper, and C. A. Ross, "Optical and Magnetic properties of γ- Iron Oxide Made by Reactive Pulsed Laser Deposition," IEEE Trans. Magn. **39**(5), 3172–3174 (2003).
23. T. Hirano, H. Hotaka, E. Komuro, T. Namikawa, and Y. Yamazaki, "Magnetic and magneto-optical properties of Ca-doped Bi:YIG sputtered films," IEEE Trans. Magn. **28**(5), 3237–3239 (1992).
24. S. J. Zhang, X. Y. Guo, F. P. Zhang, C. L. Xu, F. L. Shi, H. W. Zhang, Z. Y. Zhong, and B. J. Guo, "Effects of rapid recurrent annealing on structure and magneto-optical properties of garnet films," J. Appl. Phys. **73**(10), 6832–6834 (1993).
25. H. S. Kim, Y. H. Lee, and S. S. Lee, "Grain Size Control of Bi-substituted Garnet Films Crystallized by Multi-Step Rapid Thermal Annealing for Magneto-Optical Disks," Jpn. J. Appl. Phys. **32,** L1804–L1807 (1993).

1. Introduction

Control of light at nanometre spatial scale and modulating it at tens of gigahertz is currently a very challenging task. In this respect, magneto-optical (MO) effects are very promising as they allow fast modulation of light polarization and intensity via external magnetic fields. Bismuth-substituted iron garnet (Bi:IG) compounds are known to be the best class of magneto-optical materials for use in various MO devices and magnetic photonic crystals (MPC) [1–18]. Moreover, several new Bi:IG based structures for nanophotonics applications have been suggested and investigated recently, e.g. magnetic plasmonic heterostructures [16]. However, the practical use of Bi:IG materials in photonic devices is currently limited to bulk-optic isolators. In the visible spectral range, the optical absorption of RF magnetron sputtered, ion beam sputtered and pulsed laser-deposited (PLD) high-bismuth-content garnet films is very high, and is typically measured to be in the range of $3\text{-}5 \times 10^3$ cm^{-1} at 633 nm [3,13]. The maximum specific Faraday rotation so far reported was $\Theta_F = 8.09°/\mu$m at 633 nm, but unfortunately, there was no data reported on the optical properties of these films [5,6].

The RF magnetron sputtered garnet films are extremely attractive for practical device development applications, since the sputtering procedure is most suitable for the integration of Bi:IG films into optical components and devices, and allows precise in situ high-resolution thickness measurement due to relatively slow growth rates. However, the high optical absorption losses across the visible spectral range and the absence of uniaxial magnetic anisotropy typical of sputtered high-bismuth-content garnet films (with compositions close to Bi$_3$Fe$_5$O$_{12}$) significantly limit the potential of Bi:IG materials in practical integrated-optics applications.

Previous analyses have shown that most of RF-sputtered Bi-substituted iron garnet films produced so far likely possess an excess of Fe content in comparison with their nominal stoichiometric compositions, for example, Bi$_3$Fe$_5$O$_{12}$. It is well known that iron oxides demonstrate a rather high absorption, for example, the optical absorption coefficient of Fe$_3$O$_4$ films exceeds 10^4 cm^{-1} [21], and that of γ-Fe$_2$O$_3$ PLD films exceeds 7×10^4 cm^{-1} [22] at 633 nm. It is obvious that the presence of even several percent of excess Fe$_2$O$_3$ or Fe$_3$O$_4$ content residing outside the garnet grains can dramatically increase the absorption losses in RF-

sputtered doped iron garnet films. Based on this hypothesis, we have fabricated and characterized several batches of co-sputtered $(Bi,Dy)_3(Fe,Ga)_5O_{12}$: Bi_2O_3 garnet-oxide composites containing various volumetric fractions of excess Bi_2O_3. As a result of our extensive characterization work, we now report a substantial improvement in MO figure of merit of sputtered $Bi_2Dy_1Fe_4Ga_1O_{12}$ and $Bi_2Dy_1Fe_{4.3}Ga_{0.7}O_{12}$ films across most of the visible spectral range by fabricating $(Bi,Dy)_3(Fe,Ga)_5O_{12}$: Bi_2O_3 composites using RF co-sputtering followed by the conventional oven annealing in air atmosphere.

2. Results and data analysis

In order to achieve the necessary level of uniaxial magnetic anisotropy in RF sputtered films (which leads to perpendicular magnetization and the desirable magnetic memory properties), the base garnet composition $Bi_2Dy_1Fe_4Ga_1O_{12}$ was selected [17], in which the gallium doping diminishes the saturation magnetization, and the dysprosium substitution increases the magnetostriction coefficient. The influence of these extra dopants reduces the specific Faraday rotation Θ_F to - 2°/μm from about - 6.3°/μm, estimated using a linear approximation for the compositions $Bi_x(YLu)_{3-x}Fe_5O_{12}$ to the ultimate composition $Bi_3Fe_5O_{12}$ [7]. At the same time, the reduction in Bi content and the dilution of magnetic sublattices results in smaller optical absorption, so the MO figure of merit $2\Theta_F / α$ for $Bi_2Dy_1Fe_4Ga_1O_{12}$ can be practically the same as that for $Bi_3Fe_5O_{12}$. There have been rather many reports on the observations of an excess of iron content in RF-sputtered garnet films in comparison with the stoichiometry of $(BiDy)_3(FeGa)_5O_{12}$, for example, the synthesis of garnet films having the measured averaged stoichiometry of type $Bi_{1.2}Dy_{1.3}Fe_{4.4}Ga_{1.1}O_{12}$ has been reported [9]. Based on our hypothesis that excess iron oxides residing outside garnet grains may be responsible for the increased absorption of sputtered films compared with monocrystalline garnets, we investigated the influence of excess bismuth oxide content in RF-sputtered films on their optical and MO properties by co-sputtering the compositions $Bi_2Dy_1Fe_4Ga_1O_{12}$ and also $Bi_2Dy_1Fe_{4.3}Ga_{0.7}O_{12}$ with extra Bi_2O_3 from a separate target.

The sputtering targets used were 3" oxide-mix-based targets of nominal stoichiometries $Bi_2Dy_1Fe_4Ga_1O_{12}$, $Bi_2Dy_1Fe_{4.3}Ga_{0.7}O_{12}$ and Bi_2O_3, and co-sputtered garnet-oxide composites with extra Bi_2O_3 content of up to an estimated 50% of film's total volume were fabricated. Several batches of composites were deposited onto glass and GGG (111) substrates with the thicknesses between 500 – 1500 nm, using low-pressure (1 mTorr) Ar plasma and substrate temperatures of 250 °C. As-deposited films were amorphous, and post-deposition annealing was performed inside an oven at temperatures between 480 and 700 °C, dependent on the excess Bi_2O_3 content. The properties of our high-Bi-content composite garnet-oxide films are extremely attractive for MO applications. The excess Bi_2O_3 content in the composite films results in the reduction of the optical absorption in both the amorphous and polycrystalline phases. The lowest possible absorption coefficients achieved in our composite films at 635 nm were about 1100-1200 cm^{-1}, which is comparable with the best absorption achievable in epitaxial monocrystalline garnet layers fabricated using liquid-phase epitaxy (LPE) [2]. At the same time, significantly increased specific Faraday rotations were measured across the visible and near-infrared ranges in several garnet-oxide composites in comparison with these measured in doped garnets sputtered without adding any excess bismuth oxide content. Very high quality epitaxial garnet films have previously been manufactured using the technique known as sputter epitaxy [4], which requires rather precise matching of the lattice parameters between the garnet layers and substrates and is also very critical with respect to the selection of the substrate temperatures during the deposition process. During our study, we concentrated on achieving low optical absorption simultaneously with high Faraday rotation in the visible spectral range using conventional RF magnetron sputtering. The goal was to achieve the combination of properties suitable for the magnetic constituents of 1-D MPC structures whilst avoiding any stringent requirements in relation to the substrate type and substrate temperature selection.

2.1 Sputtering/annealing processes and typical process parameters

Bismuth-substituted (Dy,Ga)-doped iron garnet films were prepared on glass (Corning 1737) and (111)-oriented polished monocrystalline $Gd_3Ga_5O_{12}$ (GGG) substrates by conventional RF magnetron sputtering in low-pressure argon plasma under the process conditions specified in Table 1.

Table 1. Typical sputtering conditions for magneto-optic garnet layers and garnet-oxide composites

Deposition process parameters	Values/comments
Oxide-mix based garnet targets stoichiometry	$Bi_2Dy_1Fe_4Ga_1O_{12}$ and $Bi_2Dy_1Fe_{4.3}Ga_{0.7}O_{12}$ (Kurt J. Lesker Co.)
Sputter gas	Ar, P(total) = 1 mTorr. No oxygen input.
Base pressure	P(base) < 1-2E-06 Torr (high vacuum)
RF power densities	$3.3 – 7$ W/cm^2 (150-320 W, 3'' targets) – garnets; $0.44 – 0.88$ W/cm^2 or $1.3 – 3.9$ W/cm^2 (20-40 W or 60-180 W, 2 different 3'' targets) – Bi_2O_3.
Deposition rates	3.5-8.7 nm/min (garnets) 1.2-5.4 nm/min (Bi2O3)
Substrate temperatures during deposition	250 ºC
Substrate stage rotation rate (rpm)	30
Target-to-substrate distance	18 ±2 cm
Sputtering system model and description	KVS-T4065 (Korea Vacuum Technology Ltd), down-sputtering type, three RF guns for 3'' targets, with independently-activated shutters at all guns and above the substrate stage.
Geometry and disposition of magnetron sources	In the vertical plane, the directions normal to the sputtering target surfaces form 30° angles with the normal to the (horizontal) substrate stage surface. In the horizontal cross-section passing through the target centers, the target centers are at the vertices of an equilateral triangle having side dimension of about 150 mm.

The post-deposition annealing processes were run inside a conventional temperature-controlled and heating rate-controlled oven (Sentrotech Inc.) in air, in the range of temperatures between 620 and 720 °C for garnet compounds and between 480 and 640 °C for garnet-oxide composites. Typical annealing process duration was about 1 hour, preceded and followed by linear temperature-ramp processes during which the heating and cooling rates did not exceed 5 °C/min.

The sputtering target with composition $Bi_2Dy_1Fe_4Ga_1O_{12}$ was chosen because the films of this stoichiometry possessed simultaneously a rather high Faraday rotation and the necessary level of uniaxial magnetic anisotropy to orient the magnetization of the films in the direction perpendicular to the film plane, leading to excellent magnetic memory properties [17].

2.2 Measurements of the physical layer thickness, the absorption coefficient and specific Faraday rotation spectra

The physical thicknesses of all deposited film layers were measured in situ in real-time during the deposition processes, using a custom-made laser reflectometer system of our design, which was working in tandem with a quartz crystal microbalance pre-calibrated by using the same reflectometer. During multiple post-deposition tests of the real-time thickness measurement accuracy performed using FIB-prepared cross-sections of deposited layers and scanning electron microscopy (SEM), the physical layer thicknesses measured by SEM were always very close (within maximum 4-5% of error) to the thicknesses obtained from our real-time reflectometer. We have also developed specialized thickness-fitting software allowing

the derivation of physical layer thicknesses of single-layer films using their measured transmission spectra and the spectral data for the real part of the layer's refractive index [19]. The independent derivation of the physical thicknesses of the deposited garnet layers was performed on all samples by closely matching all measured transmission spectrum features of films to their theoretically-predicted transmission spectra, whilst accounting for the spectral dependencies of the refractive index and using absorption coefficient data measured for typical $Bi_2Dy_1Fe_4Ga_1O_{12}$ layers. The predicted transmission spectra were calculated (together with the predicted Faraday rotation spectra) using 4x4 transfer matrix method [20]. The amorphous-phase (as deposited) films spectra were fitted using the dispersion data measured in amorphous garnet layers, and the fitting of annealed films spectra involved using the index dispersion data of annealed layers. The modeled thicknesses were varied iteratively using custom-designed thin-film modeling and analysis software developed at the Electron Science Research Institute, ECU-Australia, until the modeled transmission spectra very closely matched those measured with Beckman Coulter DU 640B UV-visible spectrophotometer. A typical result of spectrally matching the modeled and measured transmission spectra of garnet films is shown in Fig. 1(a). The purpose of performing this software-assisted spectral fitting of the individual samples' thicknesses was to exclude any additional uncertainties in the layer thickness values arising due to the slight non-uniformities in the deposited thickness existing between the different samples from the same batch. These spectrally-fitted values of the physical thickness were always very close (within 5% of error) to the in situ measured thicknesses. The spectrally-fitted thickness values were then used for the determination of the specific Faraday rotation observed in our samples and were also used to derive their absorption coefficient spectra.

The absorption coefficient spectra of garnet composites were then derived (for films of known thicknesses inferred from spectrally matching all ripples observed in their transmission spectra (Fig. 1(b)), this method was confirmed by SEM cross-sectional imaging to be accurate to within at least ± 3-4%) by obtaining the exact fitting (within 0.01%) of the measured and modeled transmission spectra whilst varying the absorption coefficients at every wavelength computationally. This approach to deriving the absorption coefficient spectra of garnet-oxide composite samples, in our experience, works reliably to within an estimated ± 5% accuracy (provided that all samples tested belonged to the same class of materials and had a similar chemical composition, microstructure, and therefore did not have any significant differences in their refractive index spectrum $n(\lambda)$ from that of the ellipsometrically-measured, reliably-known index spectrum of $Bi_2Dy_1Fe_4Ga_1O_{12}$). For $Bi_2Dy_1Fe_{4.3}Ga_{0.7}O_{12}$ films and also for all composite garnet films with moderate (less than 30 – 40%) volumetric fractions of excess bismuth oxide (a material having a refractive index spectrum similar to that of our garnets and composites), we can expect that garnet-oxide composites do not show any significant (more than 1-2%) differences in their refractive index spectra from the index spectrum of $Bi_2Dy_1Fe_4Ga_1O_{12}$. The latter assumption was confirmed experimentally by measuring the transmission spectra of multiple batches of composite garnet films deposited onto both GGG and glass substrates, before and after annealing, without noticing any substantial changes in the amplitudes of the transmission ripples observed across the spectral window between 500 and 1100 nm. For all well-annealed, high-quality composite garnet samples not showing any signs of material decomposition, the fitted absorption spectra did not contain any significant non-physical ripples which could originate from the fitting inaccuracies if any noticeable changes in the material's refractive index spectrum had occurred (as has been observed in some of the highly-oxide-substituted or over-annealed samples which often showed signs of material decomposition after annealing). It is important to note that the absorption coefficients of our materials are in fact smaller than those derived, since the effects of light scattering throughout the samples' volume, on surface irregularities and on the magnetic domain boundaries in annealed films have also been contributing to the transmission loss.
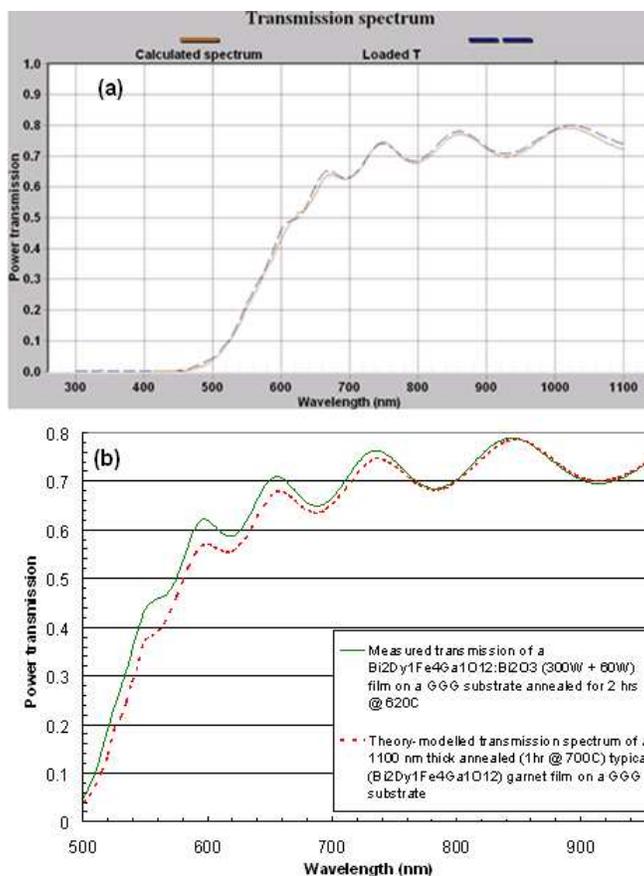
Fig. 1. (a) A typical comparison of the measured transmission spectrum of a garnet ($Bi_2Dy_1Fe_4Ga_1O_{12}$) film on a GGG substrate (blue dashed line) and its modeled transmission spectrum (continuous brown line), where the material's refractive index dispersion has been measured and fully accounted for in the model. The fitting of the actual film's thickness was performed by closely matching all measured transmission spectrum features to the modeled spectrum, whilst iteratively varying the modeled thickness. (b) The thicknesses of composite films having different absorption spectra were derived by spectrally matching the transmission ripples' minima and maxima. The differences in the absorption coefficient spectra between $Bi_2Dy_1Fe_4Ga_1O_{12}$ and $Bi_2Dy_1Fe_4Ga_1O_{12}$: Bi_2O_3 were responsible for the differences in the transmission loss observed in the visible range. The absorption coefficient spectra of composites were derived by obtaining the exact fit (fit tolerance 0.01%) between the measured and modeled transmission spectra whilst varying the absorption coefficient at each wavelength computationally, after the spectral locations of all transmission ripples were matched during the thickness fitting. The data shown was used to derive the absorption spectrum shown in Fig. 5, trace 2.

The results of optical and MO characterization of our garnet films indicate that they possess a combination of properties which is highly suitable for use in the magnetic component layers of MPC structures which require MO materials with low optical absorption.

Figure 2 shows a summary of absorption coefficient changes across the visible and near-infrared regions that occur in garnets and garnet-oxide composite films during the annealing (crystallization) processes and also shows the superior, low-absorption performance of some of the composite garnet-oxide formulations in comparison with undiluted garnets.
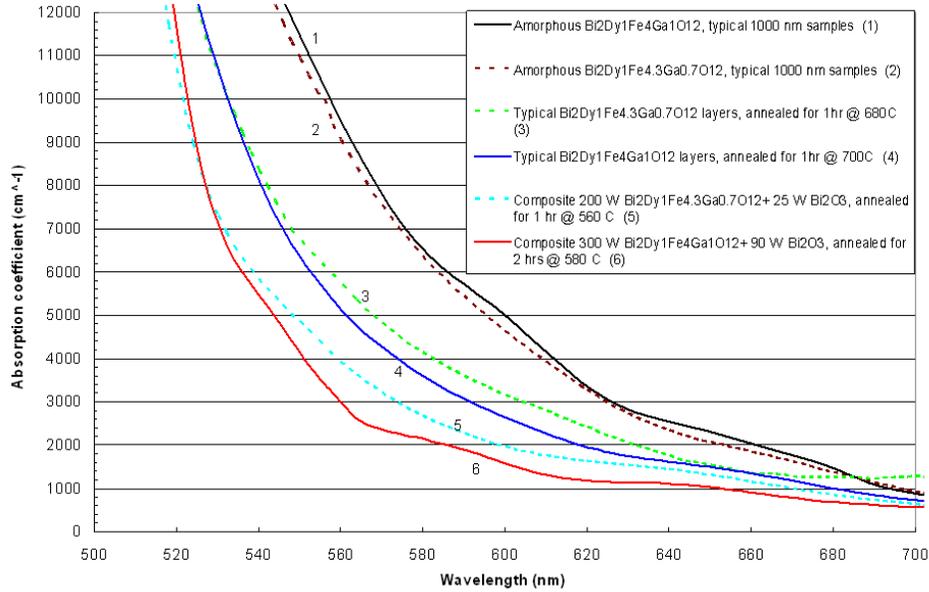
Fig. 2. Derived absorption coefficients spectra of sputtered $Bi_2Dy_1Fe_4Ga_1O_{12}$ and $Bi_2Dy_1Fe_{4.3}Ga_{0.7}O_{12}$ layers on GGG(111) substrates (in their amorphous and polycrystalline phases) and these of the best-performing annealed composite garnet films prepared using co-sputtering, with the main sputtering and annealing process parameters specified.

As was expected, the addition of extra bismuth oxide content led to the increased transparency of as-deposited (amorphous-phase) films. Figure 3 shows the absorption coefficient spectra (derived from the measured transmission spectra) of various amorphous-phase material compositions (defined by using the RF powers supplied to the garnet and oxide targets) deposited.
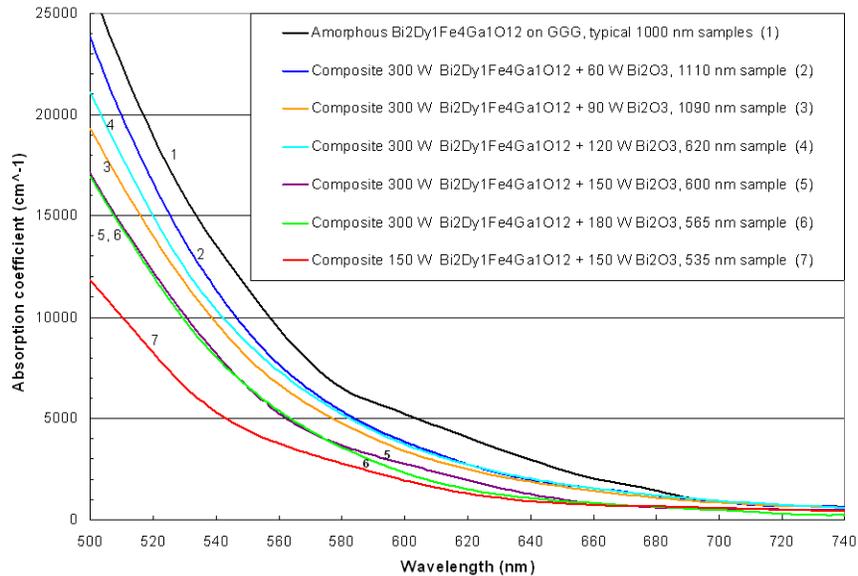
Fig. 3. Derived absorption coefficients spectra of sputtered $Bi_2Dy_1Fe_4Ga_1O_{12}$ and various $Bi_2Dy_1Fe_4Ga_1O_{12}:Bi_2O_3$ co-sputtered composite layers on GGG(111) substrates (in the amorphous phase, as deposited at the substrate temperature 250 °C). The main sputtering process parameters and film thicknesses are shown.

Since the typical ranges of crystallization temperatures so far reported in the literature as suitable for obtaining ferrimagnetic garnet-phase compounds were above at least 450 °C, we could expect that our materials deposited at 250 °C were amorphous. No measurable Faraday rotation was detected in as-deposited layers of either the "undiluted" garnets or any of the garnet-oxide composites. The amorphous structure of $Bi_2Dy_1Fe_4Ga_1O_{12}$ layers deposited at the substrate temperature of 250 °C has been confirmed in our previous study [18]. Garnet materials only exhibit MO properties if at least a fraction of the layer's volume has been crystallized into ferrimagnetic garnet phase. High-resolution images of nanocrystallites (grains) observed by TEM in the annealed layers of $Bi_2Dy_1Fe_4Ga_1O_{12}$ have also been reported in [18].
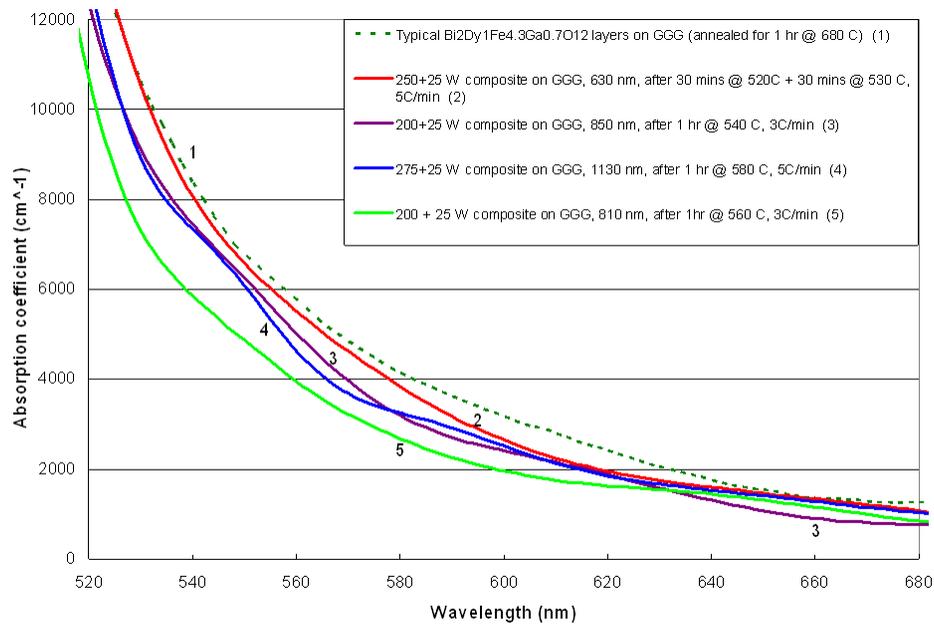
Fig. 4. Derived absorption coefficients spectra of sputtered $Bi_2Dy_1Fe_{4.3}Ga_{0.7}O_{12}$ and of several co-sputtered garnet composite layers of type $Bi_2Dy_1Fe_{4.3}Ga_{0.7}O_{12}:Bi_2O_3$ on GGG(111) substrates after annealing at the temperatures indicated. The main sputtering/annealing process parameters and also the derived film thicknesses are shown.

Figures 4-6 show the fitted absorption coefficient spectra of a range of garnet-oxide composites synthesized on two different substrate types (GGG(111) and Corning 1737 glass) obtained after running various annealing processes. The absorption spectra of optimally-annealed undiluted garnet layers of the same composition type are also shown for comparison. It is evident that, for a range of annealed composite garnet types, a significant reduction in the optical absorption coefficients is demonstrated across most of the visible and near-infrared spectral ranges.
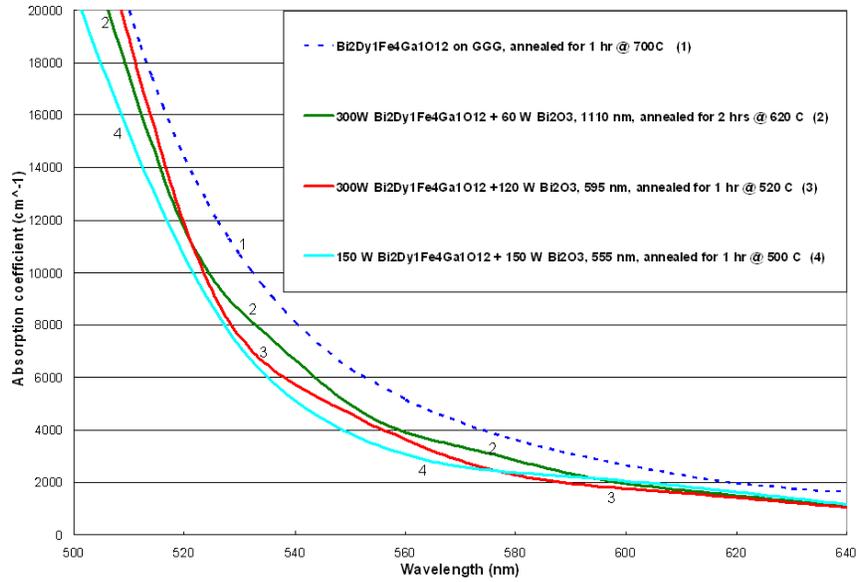
Fig. 5. Derived absorption coefficients spectra of sputtered $Bi_2Dy_1Fe_4Ga_1O_{12}$ and of several co-sputtered garnet composite layers of type $Bi_2Dy_1Fe_4Ga_1O_{12}:Bi_2O_3$ on GGG(111) substrates after annealing at the temperatures indicated. The main sputtering process parameters and film thicknesses are also shown.
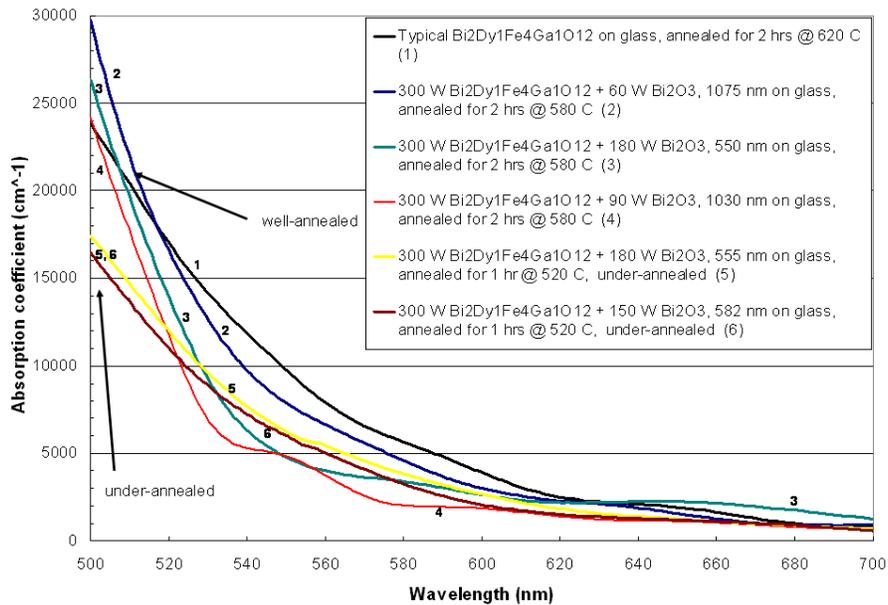

Fig. 6. Derived absorption coefficients spectra of sputtered $Bi_2Dy_1Fe_4Ga_1O_{12}$ and of several co-sputtered garnet composite layers of type $Bi_2Dy_1Fe_4Ga_1O_{12}:Bi_2O_3$ on Corning 1737 glass substrates after annealing at the temperatures indicated. The main sputtering process parameters and film thicknesses are also shown.

The specific Faraday rotation spectra of our garnets and some of the best-performing composite films are shown in Fig. 7. It was found that the co-sputtered materials have shown a stronger Faraday rotation than the typical garnet films, for a range of composite materials

synthesized, and at the same time possessed a lower absorption and a near-100% remnant magnetization. The specific Faraday rotations peaked at some fractions of added bismuth oxide content, probably due to the stronger Bi substitutions achieved within garnets' dodecahedral sublattice, and then decreased as the growing Bi_2O_3 content within the composite films likely reduced the volumetric fraction of the garnet phase within the film layers. These preliminary hypotheses still need to be investigated in detail using methods of transmission electron microscopy and elemental microanalysis.

The highest values of specific Faraday rotation obtained in our composite films were more than $10°/\mu m$ at 532 nm, $2.6°/\mu m$ at 635 nm, and $1.9°/\mu m$ at 670 nm, which lead to almost doubling the MO quality of the typical (undiluted, obtained by sputtering the garnet targets only) garnet layers in the visible range whilst still retaining their useful magnetic memory properties (near-square hysteresis loops). The best MO figure of merit $(2\Theta_F/\alpha)$ of our composite films measured so far at 635 nm was $43°(+/–2°)$, which makes our synthesized materials very attractive for nano-structured magneto-photonic components and devices.
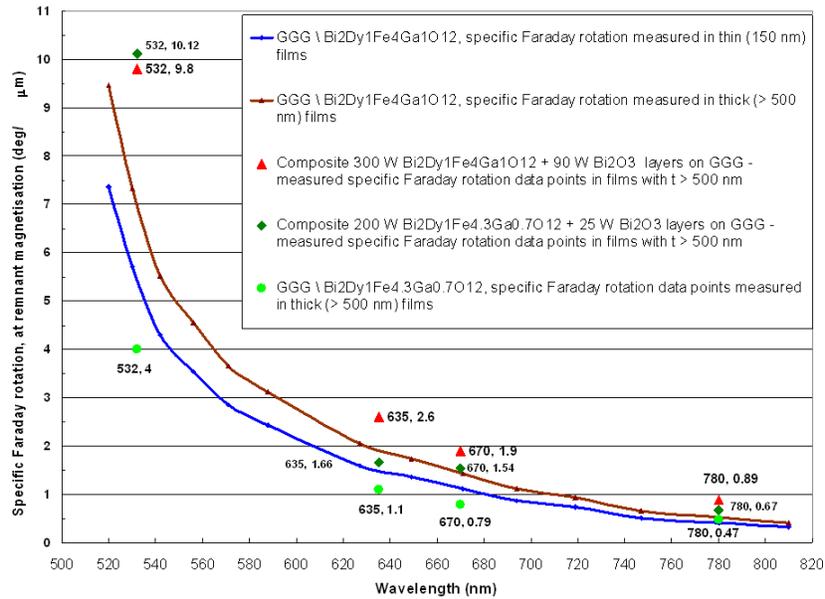

Fig. 7. Specific Faraday rotation (measured at remanent states of magnetization, as a "one-way" angle) of typical $Bi_2Dy_1Fe_4Ga_1O_{12}$, $Bi_2Dy_1Fe_{4.3}Ga_{0.7}O_{12}$ layers, and of the best-performing composite garnet films deposited onto GGG(111) substrates.

The observed difference between the specific Faraday rotation spectra of relatively thin and thicker (> 500 nm) garnet samples will require further analysis involving detailed studies of microstructure and chemical composition of garnet layers, as well as research into possible adjustments of the annealing regimes.

2.3 Optimization of the annealing regimes and results for the MO quality factor spectra

The selection of optimum thermal processing regimes for crystallizing Bi-substituted iron garnet layers is an area of active ongoing research [17,18,23–25]. It is important to note that, since the optimum annealing regimes of doped iron garnet compounds are extremely composition-dependent [23] (both the crystallization threshold and the material damage threshold temperatures are very sensitive to the number of Bi atoms per unit formula), we were so far unable to optimize the thermal processing regimes for all of the composite garnet batches synthesized, and a number of sample batches remained either under-annealed (not showing any significant absorption spectrum modification after annealing and showing either no Faraday rotation or very small MO quality), or over-annealed, despite multiple attempts to

find suitable annealing temperatures and process durations. In the "over-annealed" state, the samples typically showed significant scattering of the transmitted light due to a combined effect of the surface roughening and numerous cracks propagating throughout the samples' volume. Interestingly, in many of the "over-annealed" samples, the specific Faraday rotations measured at 635 and 532 nm were found to be very close to, or even exceeding, those measured in the best annealed samples of the same material type. On the other hand, quite often (but not always), the specific Faraday rotations measured in the composite garnet samples annealed for 1-2 hours at a selected temperature were significantly (up to 25-50%) smaller than those obtained after just 30 minutes of annealing at the same temperature. These results suggest that the loss of bismuth content and/or material decomposition processes, as well as the formation of different (non-garnet) material phases (for example, $BiFeO_3$ or $Bi_2Fe_4O_9$ [15]) also did play a role.

Our research is ongoing into the optimization of the thermal processing regimes of various doped iron garnet compounds and especially of the garnet-oxide composite materials. As was expected, with the increasing content of bismuth within the composite samples, the annealing temperatures were decreasing and the "thermal processing windows" of the materials became much narrower. The microstructural properties, the chemistry and crystal structure of the garnet nanocrystallites likely formed within the composite materials so far synthesized will be studied separately. The increased specific Faraday rotations measured within some composites at a number of wavelengths do suggest that some of the excess bismuth atoms were incorporated into the dodecahedral sublattices of the likely resulting garnet nanocrystals, thus increasing the number of Bi atoms per unit formula. However, further investigations will be necessary to either confirm or deny this hypothesis. The chemical make-up of the film volumes located in-between the garnet grains possibly formed within the composites will also be studied using the energy-dispersive X-ray spectral analysis. So far, we have only studied the microstructural properties and elemental compositions of garnet films and all-garnet multilayers sputtered without adding extra bismuth oxide content [18,19]. As was expected, the composite materials having very large (in excess of 25-30%) volumetric contents of excess bismuth oxide demonstrated very high transparency in the amorphous phase, yet were extremely difficult to anneal without inducing the material decomposition or cracks/surface damage unless a very narrow "temperature window" was found. These films, if annealed successfully, still remained quite transparent but demonstrated rather small specific Faraday rotations, possibly due to the decrease in the volumetric fraction of the film volumes occupied by the garnet phase. Interestingly, all of the composite materials synthesized so far showed near-100% remnant magnetization, a high-contrast magnetic domains structure and therefore possessed strong perpendicular magnetic anisotropy. In other types of sputtered garnet compounds with strong Bi substitution, for example in $Bi_{2.2}Dy_{0.8}Fe_{4.5}Ga_{0.5}O_{12}$, the remnant magnetization was observed to be only about 70% of the saturation magnetization in our experiments, and $Bi_3Fe_5O_{12}$ layers are always magnetized in-plane.

A summary of different annealing temperatures and thermal processing windows found suitable for the crystallization of MO garnets and various types of garnet-oxide composites is shown in Fig. 8. The data shown is based on the multiple annealing trials performed with various batches of composite material samples followed by the optical and MO characterization of the annealed films. Our annealing experiments allowed the determination of approximate "lower boundary of the annealing range" temperatures for various composite materials synthesized. We show the "processing window boundaries" in Fig. 8 to assist other researchers in reproducing our results. The "lower boundary" and "upper limit" temperatures are shown as a guide only. Running the annealing processes at or below the "lower boundary" temperatures would, in our experience, lead to obtaining only very small specific Faraday rotations after 1 hour-long process durations. Running the annealing processes at or above the indicated "upper limit" temperatures will likely lead to material decomposition and/or significant film surface degradation.

The sample-to-sample and batch-to-batch repeatability of the resulting annealed material properties was found to be very good (in material batches for which the temperature window

boundaries have been found, as shown in Fig. 8), even though the accuracy of temperature measurement inside oven is estimated to be about ± 10 °C.
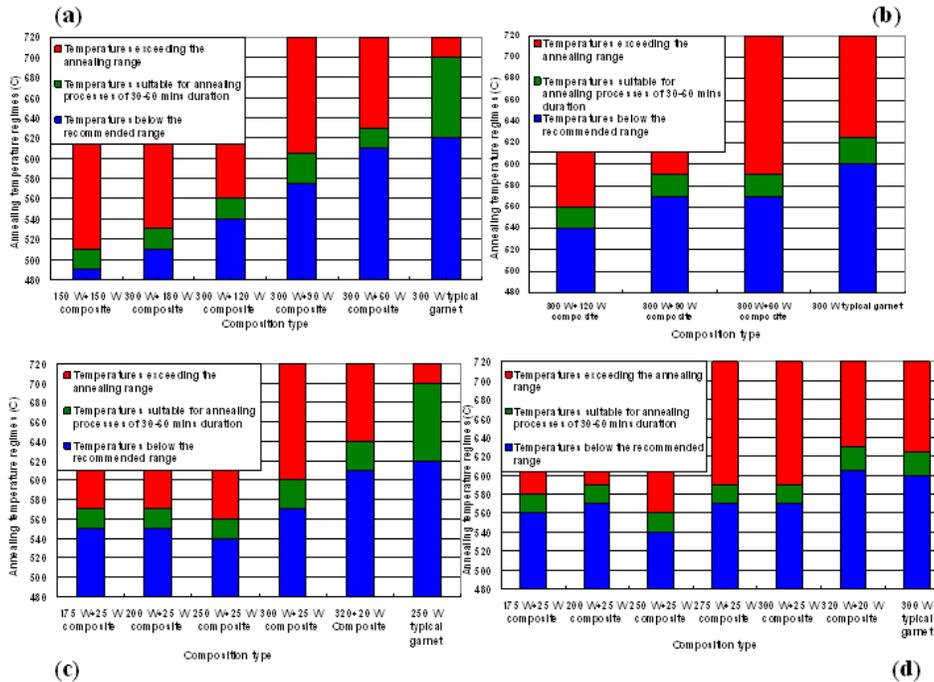

Fig. 8. Summary of annealing temperatures used for crystallizing MO garnets and various types of garnet-oxide composites. The data are shown for (a) $Bi_2Dy_1Fe_4Ga_1O_{12}$ and several $Bi_2Dy_1Fe_4Ga_1O_{12}$: Bi_2O_3 composites deposited onto GGG (111) substrates; (b) $Bi_2Dy_1Fe_4Ga_1O_{12}$ and $Bi_2Dy_1Fe_4Ga_1O_{12}$: Bi_2O_3 composites deposited onto Corning 1737 glass substrates; (c) $Bi_2Dy_1Fe_{4.3}Ga_{0.7}O_{12}$ and $Bi_2Dy_1Fe_{4.3}Ga_{0.7}O_{12}$: Bi_2O_3 composites deposited onto GGG (111) substrates; (d) $Bi_2Dy_1Fe_{4.3}Ga_{0.7}O_{12}$ and $Bi_2Dy_1Fe_{4.3}Ga_{0.7}O_{12}$: Bi_2O_3 composites deposited onto Corning 1737 glass substrates.

The films on glass substrates could not be annealed at temperatures exceeding 625-630 °C as the glass would begin to soften. Typically, the garnet and garnet-oxide composite films showed 10-15% less Faraday rotation per unit film thickness when deposited onto glass substrates. Some high-oxide-content batches, however, showed more transparency and less scattering from film surface defects after running the annealing processes, in films deposited onto glass substrates.

Figure 9 shows the measured hysteresis loops of specific Faraday rotation at 532 nm in several garnet-oxide composite films. The hysteresis loops of all garnet materials and all composites tested were found to be practically perfectly "square", with remnant magnetizations being indistinguishably close to 100% of the saturation magnetization. Some significant differences in the coercive force and switching field values have been noticed to exist in different materials; these magnetic characterization results will be further studied and reported later. Our measurements indicate a significant decrease in the coercive force and switching field values observed in some of the best-performing composite materials compared with these measured by us previously in undiluted garnet layers [17].
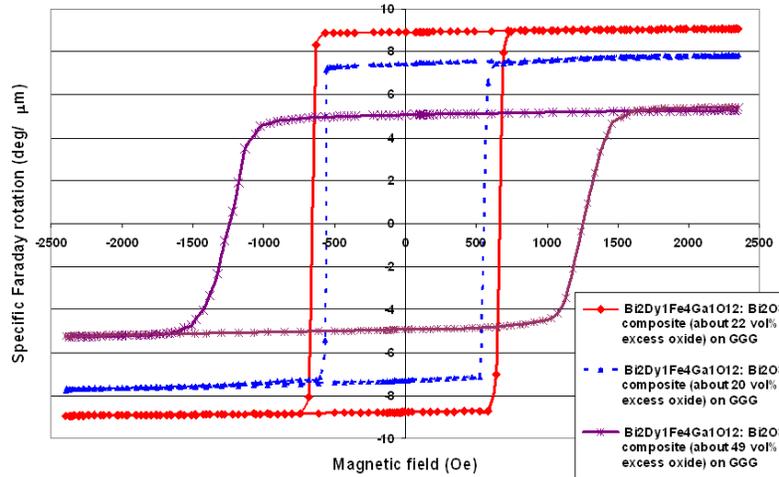
Fig. 9. Hysteresis loops of specific Faraday rotation measured at 532 nm in several Bi-substituted Ga-doped garnet-oxide composite films having thicknesses of 1.1 µm (solid red curve), 0.74 µm (dashed blue curve) and 0.555 µm (brown star curve) grown on GGG (111) substrates.

Figure 10 shows photographs of magnetic domain patterns observed in two different garnet-oxide composite films (obtained in a demagnetized state, immediately after the annealing and cooling processes) using a transmission-mode Leitz Orthoplan polarizing microscope.
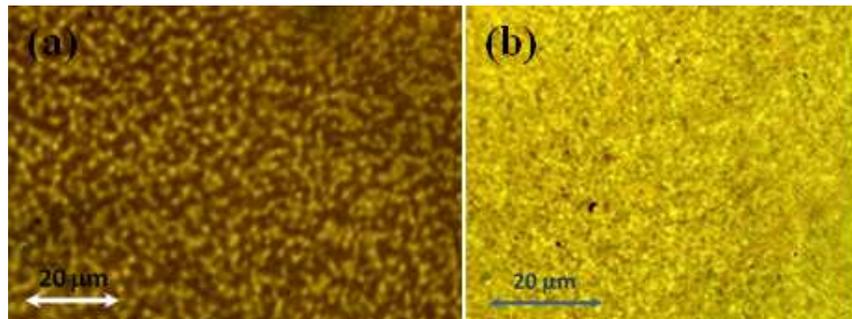

Fig. 10. Magnetic domain patterns observed using a transmission-mode polarizing microscope in two different demagnetized garnet-oxide composite films sputtered onto GGG (111) substrates (a) 1000 nm of $Bi_2Dy_1Fe_4Ga_1O_{12}$:Bi_2O_3, est. 23% excess oxide (300W + 90W), and (b) 850 nm of $Bi_2Dy_1Fe_{4.3}Ga_{0.7}O_{12}$:$Bi_2O_3$, est. 24% excess oxide (200W + 25W).

Figures 11 and 12 show the results of MO quality factor (figure of merit) measurement obtained at a discrete set of laser wavelengths with all successfully annealed garnet and garnet-oxide composite samples. The measurements of specific Faraday rotation were taken using Thorlabs PAX polarimeter system and an electromagnet, by recording the azimuth directions of the plane of polarization of light transmitted through samples magnetized into two of its remnant magnetization states (the electromagnet current was being switched off after saturating the sample's magnetization in each direction). This ensured that the Faraday rotation of the 500 µm thick GGG (paramagnetic) substrates (being as large as about ± 0.25° at 532 nm) did not affect the measurement results obtained for the film layers. The data used for calculating the error bar values were as follows: absolute error of the Faraday rotation angle measurement of ± 0.05°; relative errors in the fitted absorption coefficient values of ± 5%; relative errors of the film thickness measurement of ± 4%. The error bars show the entire range (worst-case to best-case) of the possible MO quality factor values for each data point

shown, within the measurement accuracy limitations as described. Special care was taken to measure both the transmission spectra (used for deriving the absorption spectra) and the Faraday rotation spectra within the same surface region of every sample.
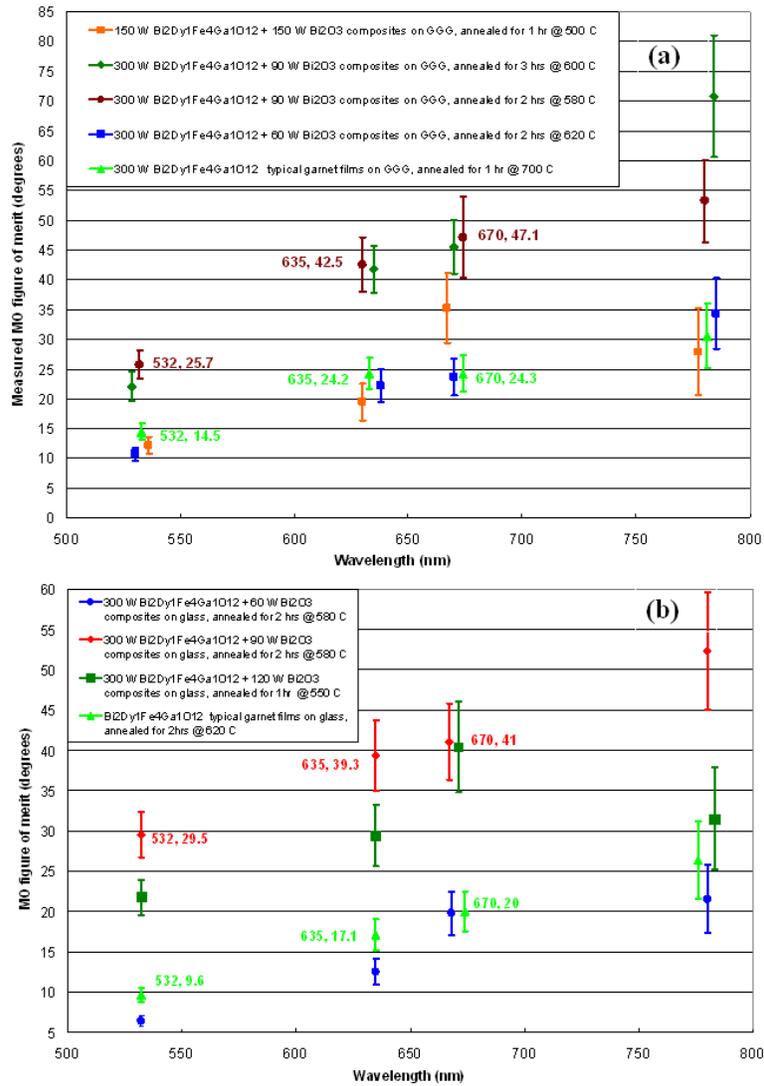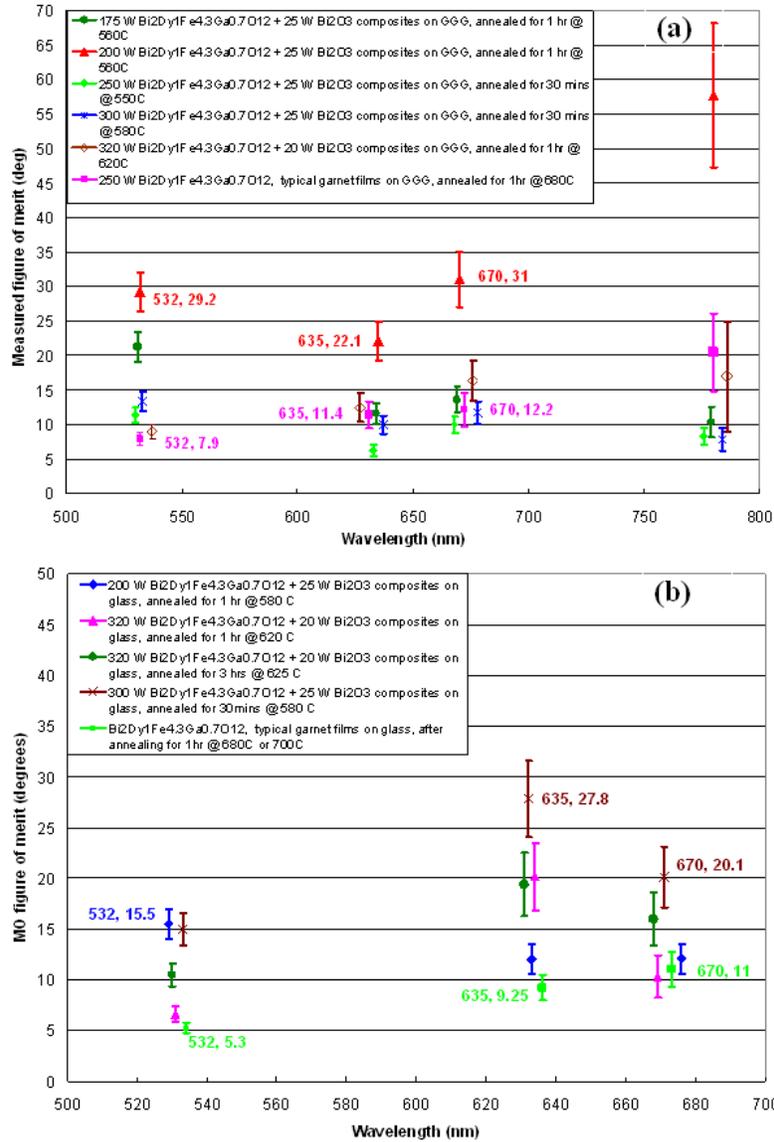

Fig. 11. Measured MO figure of merit spectra (the data points were taken at the wavelengths of 532, 635, 670 and 780 nm) of the typical $Bi_2Dy_1Fe_4Ga_1O_{12}$ layers and of various garnet composites of type $Bi_2Dy_1Fe_4Ga_1O_{12}$: Bi_2O_3 deposited onto GGG(111) (a) and Corning 1737 glass substrates (b).

Fig. 12. Measured MO figure of merit spectra (the data points were taken at the wavelengths of 532, 635, 670 and 780 nm) of the typical $Bi_2Dy_1Fe_{4.3}Ga_{0.7}O_{12}$ layers and of various garnet composites of type $Bi_2Dy_1Fe_{4.3}Ga_{0.7}O_{12}$: Bi_2O_3 deposited onto GGG(111) (a) and Corning 1737 glass substrates (b).

The composite garnet materials synthesized can be characterized (approximately) by the estimated volumetric fraction of excess bismuth oxide (originating from a separate sputtering target) within the deposited films. Measurements of partial deposition rates versus the RF source power were performed for each of the sputtering targets used, which allowed approximate quantification of the excess Bi_2O_3 fractions according to the formula excess Bi_2O_3 fraction = partial Bi_2O_3 rate / total deposition rate. Figure 13 shows the measured MO figures of merit (best obtained in our annealing experiments so far) at 532, 635 and 670 nm versus the estimated excess volumetric content of Bi_2O_3 added to our composite garnet-oxide films as a result of co-sputtering processes. It is interesting to note that the best MO quality factors achieved for both composition types peaked at the same range of excess oxide fractions (between 22 and 25 vol.%). For both garnet composition types tested, the materials

having excess oxide contents near 20 vol.% and also near 30 vol.% were extremely difficult to anneal without spoiling their optical quality, which resulted in obtaining very small MO quality factors. Surprisingly, larger MO quality factors were measured at 532 nm compared to these measured at 635 nm in some of the composite materials of type $Bi_2Dy_1Fe_{4.3}Ga_{0.7}O_{12}$: Bi_2O_3.
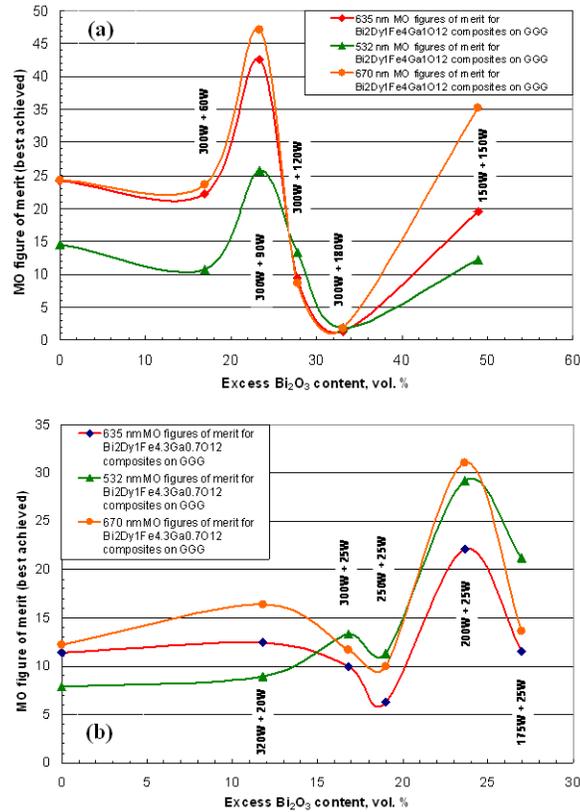

Fig. 13. Measured MO figures of merit (best obtained in our annealing experiments so far) at 532, 635 and 670 nm versus the estimated excess volumetric content of Bi_2O_3 in co-sputtered composite garnet films of types $Bi_2Dy_1Fe_4Ga_1O_{12}$: Bi_2O_3 (a) and $Bi_2Dy_1Fe_{4.3}Ga_{0.7}O_{12}$: Bi_2O_3 (b) deposited onto GGG (111) substrates.

A significant drop in the MO figures of merit of composites having the excess bismuth oxide content near 30% was due to the post-anneal surface degradation of these films, which was very difficult to avoid, and led to the appearance of significant scattering losses. The reduction in the specific Faraday rotation observed in composite films when excess Bi_2O_3 content was increased beyond about 25 vol.% was relatively gradual, for example, we measured remnant Faraday rotations of $\pm$ 4.05 °/μm at 532 nm for a batch of (150 W $Bi_2Dy_1Fe_4Ga_1O_{12}$ + 150 W Bi_2O_3) samples on GGG substrates, in which the excess bismuth oxide content was estimated to be near 50 vol.%. Thus, about half of the maximum-observed MO activity at 532 nm was measured in samples having an estimated 50 vol.% of added bismuth oxide.

3. Summary of results

A range of new MO composite garnet-oxide materials with high bismuth content were synthesized and characterized optically, magnetically and magneto-optically. The material characterization results obtained indicate that the MO quality factors of two important types of doped MO garnet materials were nearly doubled at 635 nm and 670 nm, and nearly-tripled at

532 nm, by means of synthesizing the composites possessing an excess of bismuth oxide using RF magnetron co-sputtering technology. The likely source of excess optical absorption in polycrystalline sputtered garnet layers compared with epitaxially-grown (LPE) garnet monocrystals is the existence of iron oxide phases residing outside garnet grains. The addition of extra bismuth oxide content can lead to significant improvements in the optical transparency and specific Faraday rotation of sputtered garnet materials in the visible range.

4. Conclusion

We have demonstrated composite garnet-oxide films of record-high MO quality in the visible spectral range fabricated by adding the excess Bi_2O_3 content into the garnet structure of type $(BiDy)_3(FeGa)_5O_{12}$ and characterized the composite garnet-oxide materials optically, magnetically and magneto-optically. The new synthetic materials have shown great promise for the development of next-generation integrated-optics devices requiring the functionalities based on Faraday effect and magnetic memory properties, due to the excellent MO figures of merit achieved in these materials.

The new synthetic magneto-optical materials have exhibited excellent optical and magneto-optical properties that make them attractive for visible-range and near-infrared applications, including the development of high-performance magnetic field visualizers and integrated devices for polarization control. Bi-substituted composite garnet-oxide films fabricated with excess bismuth oxide content using RF co-sputtering and conventional oven annealing processes have been found to demonstrate simultaneously record MO quality and uniaxial magnetic anisotropy.